Poly(ethylene terephthalate) Nanocomposite Fibers with Functionalized Multiwalled Carbon Nanotubes Via *In-Situ* Polymerization

Sung Jin Mun,[1] Young Mee Jung,[2] Jeong-Cheol Kim,[3] Jin-Hae Chang[1]

[1]*Department of Polymer Science and Engineering, Kumoh National Institute of Technology, Gumi 730-701, Korea*
[2]*Department of Chemistry, Kangwon National University, Chunchon 200-701, Korea*
[3]*Gwangju R&D Center, Korea Institute of Industrial Technology, Gwangju, 500-460, Korea*

Received 13 July 2007; accepted 29 December 2007
DOI 10.1002/app.28164
Published online 1 April 2008 in Wiley InterScience (www.interscience.wiley.com).

ABSTRACT: Poly(ethylene terephthalate) (PET) hybrids with newly synthesized functionalized multiwalled carbon nanotubes (MWNTs) were obtained by carrying out the *in situ* polycondensation of ethylene glycol with dimethyl terephthalic acid. The PET hybrids were melt-spun to produce monofilaments with various functionalized MWNT contents and draw ratios (DRs). The thermomechanical properties and morphologies of the PET hybrid fibers were determined using differential scanning calorimetry (DSC), thermogravimetric analysis (TGA), wide angle X-ray diffraction (XRD), electron microscopy (SEM and TEM), and a universal tensile machine (UTM). The XRD analysis and TEM micrographs show that the levels of nanosize dispersion can be controlled by varying the MWNT content. It was found that the addition of only a small amount of functionalized MWNTs was sufficient to improve the properties of the PET hybrid fibers. The maximum enhancement in the ultimate tensile strength was found to arise at a functionalized MWNT content of 0.5 wt %. However, the initial modulus was found to increase linearly with increases in the functionalized MWNT loading from 0 to 1.5 wt %. The thermal properties and conductivities of the PET hybrid fibers were found to be better than those of pure PET fibers. J Appl Polym Sci 109: 638–646, 2008

Key words: poly(ethylene terephthalate); multiwalled carbon nanotubes; fibers; nanocomposite

INTRODUCTION

Poly(ethylene terephthalate) (PET) is a semicrystalline polymer possessing excellent chemical resistance, thermal stability, melt mobility, and spinnability. It has been used in such diverse fields as the packaging, electrical, automotive, and construction industries.[1–3] This polymer serves as an excellent matrix for polymeric carbon nanocomposite materials.[4,5]

Nanoscale composites of polymers with carbon nanotubes (CNTs) have been studied extensively.[6–10] Nanostructured materials often possess a combination of physical and mechanical properties that are not present in conventional polymer matrix composites; because of their high aspect ratios, the presence of even low CNT concentrations can substantially improve the thermomechanical properties and electric conductivity of these materials. To achieve superior performance in CNT-filled polymer nanocomposites, there are two key issues: the dispersion of the CNTs in the polymer matrix and the interaction between the CNTs and the polymer.

CNTs are present as ropes and bundles due to their strong lateral interactions, which means that they are difficult to homogeneously disperse in a hybrid system.[8,11,12] Several methods have been used to obtain polymer nanocomposites with a homogeneous dispersion of CNTs in the polymer matrix. Melt mixing compounding, coagulation, and *in situ* polymerization are the methods usually used to prepare nanoscaled composites of polymers with CNTs. In the *in situ* polymerization method,[13–16] the CNTs are dispersed homogeneously with the monomer, then *in situ* polymerization is initiated thermally or by the addition of a suitable compound. Chain growth with the CNTs then induces CNT exfoliation and nanocomposite formation. This *in situ* polymerization technique is particularly attractive due to its versatility and compatibility with reactive monomers, and its use in commercial applications has begun.

One of the best methods for achieving the homogeneous dispersion of CNTs in a polymer matrix is the functionalization of the CNTs.[17–20] The best approach is then obviously to functionalize the CNTs with polymers that are structurally close to

Correspondence to: J.-H. Chang (changjinhae@hanmail.net).

Contract grant sponsor: Korean Government (MOST, Korea Science and Engineering Foundation (KOSEF)); contract grant number: ROI-2007-000-20353-0.

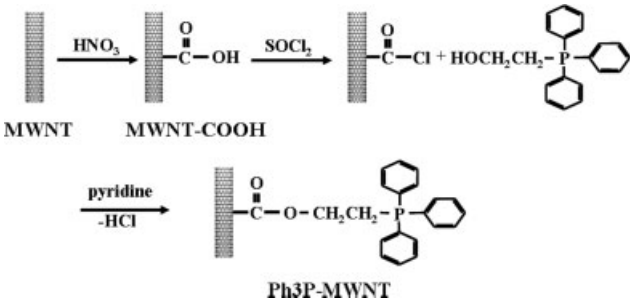

Scheme 1 Synthetic routes for the functionalized MWNT.

the matrix polymer, because such functionalization ensures the compatibility of the dispersed CNTs with the polymer matrix and limits any microscopic phase separation in the nanocomposites.

The objective of this study was to evaluate the effects of varying the functionalized multiwalled carbon nanotube (MWNT) content of the PET nanocomposites. In this article, we introduce a newly synthesized functionalized MWNT that can be used in PET hybrid systems, and also describe a method for fabricating PET hybrids via *in situ* polymerization. The thermomechanical properties, electrical conductivities, and morphologies of the resulting fibers of PET hybrids with various functionalized MWNT contents and draw ratios (DRs) are reported.

EXPERIMENTAL

Materials

All reagents were purchased from TCI, Junsei Chemical (Tokyo, Japan), and Aldrich Chemical (Seoul, Korea). Commercially available solvents were purified using distillation. MWNTs (Iljin Nanotech, Seoul, Korea) synthesized with a thermal chemical vapor decomposition method were treated with acid in a sonication bath prior to use to ensure high levels of dispersion.

Preparation of the functionalized MWNTs: Ph3P-MWNT

Purified MWNTs were obtained after a soft-bake at 250°C for 24 h, then sonication was carried out in concentrated HNO_3 at 80°C for 20 min to produce MWNT-COOH. The carboxylic acid groups can be converted into acyl chloride groups through treatment with thionyl chloride ($SOCl_2$). The acyl chloride-terminated MWNTs (MWNT-COCl) are then susceptible to reaction with alcohols to produce esters. About 2.0 g of MWNT-COOH was stirred in 100 mL of $SOCl_2$ at 70°C for 48 h. After the excess $SOCl_2$ had been removed by using anhydrous tetrahydrofuran (THF), a mixture of 0.2 g MWNT-COOH and 20 g (0.05 mol) of (2-hydroxyethyl) triphenyl phosphonium bromide in excess pyridine was heated at 130°C for 12 h. After cooling to room temperature, the excess pyridine was removed by washing with acetone. The remaining solid was washed several times with a water/ethanol mixture. The resulting black solid was dried at room temperature under vacuum. The synthetic route for the functionalized MWNTs, Ph3P-MWNT, is as shown in Scheme 1.

Preparation of the Ph3P-MWNT/PET hybrids

All the samples were prepared as melts. Since the synthetic procedures for the hybrids were very similar, only a representative example, the procedure for the preparation of the hybrid containing 0.5 wt % Ph3P-MWNT, is described here. About 62 g of 1,2-ethylene glycol (EG) (1.0 mol) and 0.98 g of Ph3P-MWNT were placed in a polymerization tube, and the mixture was stirred for 12 h at room temperature. About 97 g of dimethyl terephthalate (DMT) (0.5 mol) and a few drops (1.2×10^{-4} mole) of isopropyl titanate were placed in a separate tube, and this mixture was added to the Ph3P-MWNT/EG system with vigorous stirring to obtain a homogeneously dispersed system. This mixture was heated for 1 h at 190°C under a steady stream of N_2 gas. The temperature of the reaction mixture was then raised to 230°C, and that temperature was maintained for 3 h under a steady stream of N_2 gas. During this period, the continuous generation of methanol was observed. Finally, the mixture was heated for 2 h at 280°C at a pressure of 1 Torr. The product redundant was cooled to room temperature, repeatedly washed with water, and dried under a vacuum at 70°C for 1 day to obtain the PET hybrid. The polymers are soluble in mixed solvents, so the mixed solvent phenol/1,1,2,2-tetrachloroethane (w/w = 50/50) was used in the measurement of solution viscosity. The inherent solution viscosities (see Table I) were found to range from 0.96 to 1.02.

TABLE I
Thermal Properties of Ph3P-MWNT/PET Hybrid Fibers

Ph3P-MWNT wt %	I.V.[a]	T_g, °C	T_m, °C	T_D^{ib}, °C	wt_R^{600c}, %
0 (pure PET)	1.02	71	245	370	1
0.3	0.96	76	254	400	14
0.5	0.97	76	254	401	14
1.0	0.98	77	253	400	15
1.5	0.96	77	255	399	17

[a] Inherent viscosities were measured at 30°C using 0.1 g/dL solutions in a phenol/1,1,2,2-tetrachloroethane (w/w = 50/50) mixture.
[b] Initial weight-loss temperature.
[c] Weight percent of residue at 600°C

Extrusion

The composites were pressed with 2500 kg/cm^2 for 2–3 min at 270°C on a hot press. The resulting ~0.5–mm-thick films were dried in a vacuum oven at 80°C for 24 h and then extruded through the die of a capillary rheometer. The hot extrudates were stretched through the die of a capillary rheometer (INSTRON 5460, High Wycombe, England) at 270°C and immediately drawn at constant speeds with a take-up machine to form fibers with various DRs. Pure PET and the PET hybrids were extruded into fibers with varying DRs through a capillary die, and the thermal and tensile mechanical properties of the extrudates were determined. The standard die diameter (DR = 1) was 0.75 mm. The DR was calculated from the ratio of the velocity of extrusion to the take-up speed. The mean residence time in the capillary rheometer was ~3–4 min.

Characterization

The Raman spectra were obtained using a Renishaw Raman system Model 3000 spectrometer equipped with an integral microscope (Olympus BH2-UMA). Radiation from a He-Ne laser (633 nm) was used as the excitation source. Raman scattering was detected with 180° geometry using a Peltier cooled (−70°C) charge-coupled device (CCD) camera (400 × 600 pixels).

The thermal behaviors of the hybrid fibers were studied using a DuPont model 910 differential scanning calorimeter (DSC) and a thermogravimetric analyzer (TGA) at a heating rate of 20°C/min under N_2 flow. The tensile properties of the fibers were determined using an Instron mechanical tester (Model 5564) at a crosshead speed of 5 mm/min. The specimens were prepared by being cut into fibers 50 mm in length. The experimental uncertainties in the tensile strengths and the moduli were ± 1 MPa and ± 0.05 GPa, respectively. The average of at least 10 individual determinations was obtained.

The morphologies of the fractured surfaces of the extruded hybrid fibers were investigated using a Hitachi *S*-2400 scanning electron microscope (SEM). An SPI sputter coater was used to sputter-coat the fractured surfaces with gold for enhanced conductivity. The samples were prepared for transmission electron microscopy (TEM) by putting the PET hybrid fibers into epoxy capsules and then curing the epoxy at 70°C for 24 h in vacuum. The cured epoxies containing the PET hybrids were then microtomed into 90-nm thick slices, and a layer of carbon, about 3-nm thick, was deposited onto each slice on a mesh 200 copper net. TEM photographs of ultrathin cross sections of the polymer/functionalized MWNT hybrid fibers were obtained on a Leo 912 OMEGA, Carl Zeiss, using an acceleration voltage of 120 kV. The electrical conductivities of the hybrid fibers were measured at room temperature with a two-probe method.

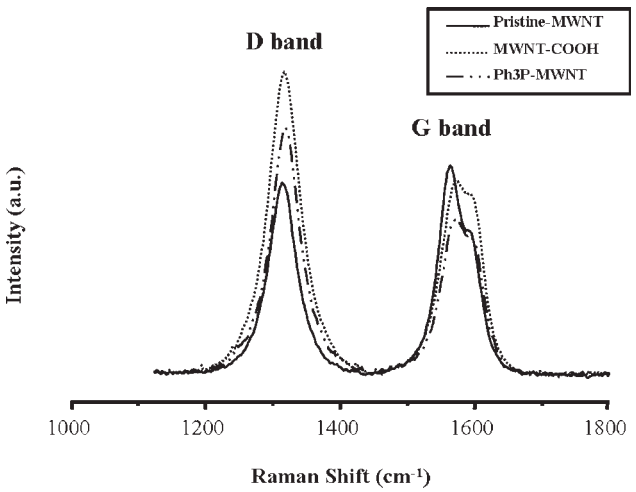

Figure 1 Raman spectra of pristine MWNT, MWNT-COOH, and Ph3P-MWNT.

RESULTS AND DISCUSSION

Raman

It is well known that Raman spectroscopy is a powerful technique for the characterization of the functionalized CNTs.[21–23] Figure 1 shows the Raman spectra of the functionalized MWNTs and the pristine MWNT starting material. Two characteristic bands, the D band (the defect or disorder mode) and the G band (the graphite or tangential mode), are present in the Raman spectra. The intensity of the D band at 1316 cm^{-1}, which is attributed to disordered sp^3-hybridized carbons in the MWNTs and to amorphous carbon, is higher for the functionalized MWNTs because of the functional groups that are covalently attached to the MWNT walls. This increase in the intensity of the D band is similar to that found for functionalized MWNTs,[21] and is in good agreement with previous reports.[22,23] The G band for the functionalized MWNTs is at 1573 cm^{-1}, whereas that for the pristine MWNTs is at 1563 cm^{-1}. The shift to higher wavenumbers of this peak with functionalization arises because the functional groups can act as electron acceptors, which results in *p*-doping of the MWNTs and a stiffening of the C—C bonds. This result provides direct evidence for changes in the graphite structure of the MWNTs due to functionalization.

The I_D/I_G ratio of the functionalized MWNTs is much higher than that of the pristine MWNTs. This increase in the I_D/I_G ratio reflects the increase in the number of crystal defects due to functionalization.

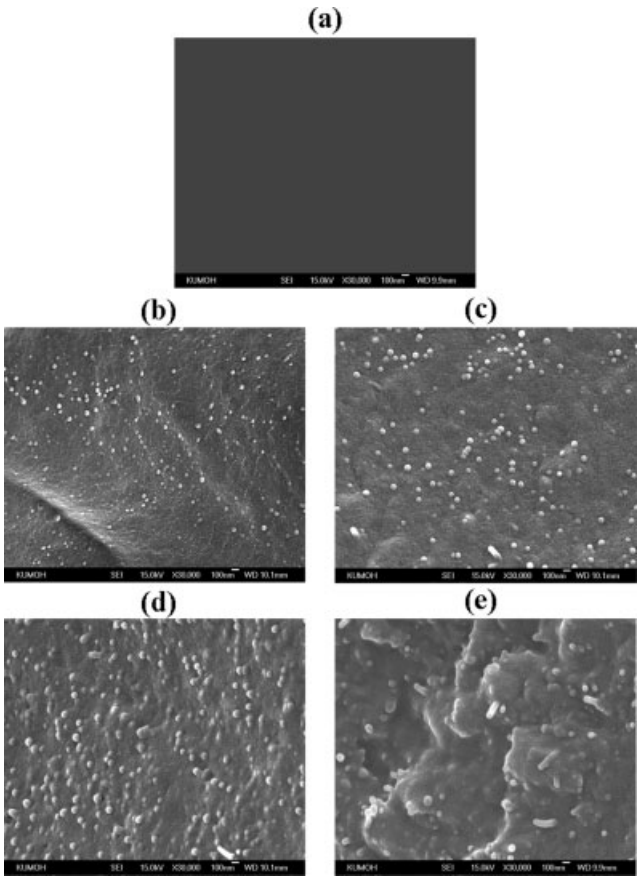

Figure 2 SEM photographs of (a) 0 (pure PET), (b) 0.3, (c) 0.5, (d) 1.0, and (e) 1.5 wt % Ph3P-MWNT in PET hybrid fibers.

Further, the *G* bandwidth is higher for the functionalized MWNTs. The increases in the I_D/I_G ratio and *G* bandwidth are indications of an increase in the number of defects in the nanotube lattice. This might be due to the introduction of covalently bound moieties into the nanotube framework, resulting in the conversion of a significant amount of sp^2-hybridized carbon to sp^3-hybridized carbon. Thus the Raman spectra provide clear evidence of the functionalization of the MWNTs.

Morphology

The morphologies of the extruded fibers obtained from the hybrids containing up to 1.5 wt % Ph3P-MWNT were determined by examining images of their fracture surfaces obtained with SEM, as shown in Figure 2. Figure 2 shows that well dispersed white spots, thought to be MWNT domains, are present in undrawn (DR = 1) PET hybrid fibers containing 0.3 and 0.5 wt % Ph3P-MWNT. The 0.3 and 0.5 wt % hybrids [Fig. 2(b,c)] contain fine MWNT phases 20–40 nm and 30–60 nm in diameter, respectively, but the Ph3P-MWNT phase in the 1.0 wt % hybrid fiber [Fig. 2(d)] is much larger, because of agglomeration. The 1.5 wt % hybrid [Fig. 2(e)] also contains MWNT particles with domain sizes 80–120 nm in diameter. The 1.5 wt % hybrid also contains voids and some deformed regions that may be due to the coarseness of the fractured surface. However, the fractured surfaces are more deformed when the hybrids contain more Ph3P-MWNT, which is probably a consequence of the agglomeration of the MWNTs. These images show that the particle size of the dispersed polymer phase increases with increases in the MWNT content. For low MWNT contents such as 0.5 wt %, the MWNTs are dispersed in the polymer matrix without the large scale agglomeration of particles. Agglomerated structures form and become denser in the polymer matrix at a MWNT content of 1.5 wt %.

Figure 3 shows micrographs of 1.5 wt % Ph3P-MWNT/PET hybrid fibers with DRs varying from 1 to 16. The particle size is almost constant up to DR = 3. However, the hybrid fiber with DR = 10 contains CNT phases almost 100 nm in diameter [see Fig. 3(c)]. The hybrid fiber with DR = 16 also exhibits fine dispersion with domains $\leq$100 nm in diameter [see Fig. 3(d)]. The domain size of the dispersed MWNT phase decreases with increasing DR. This decline in the domain size seems to be the result of excess stretching of the fibers when the extrudates pass through the capillary rheometer.

More direct evidence of the formation of true nanocomposites is provided by the TEM images of ultramicrotomed sections. Figure 4(a-c) show the

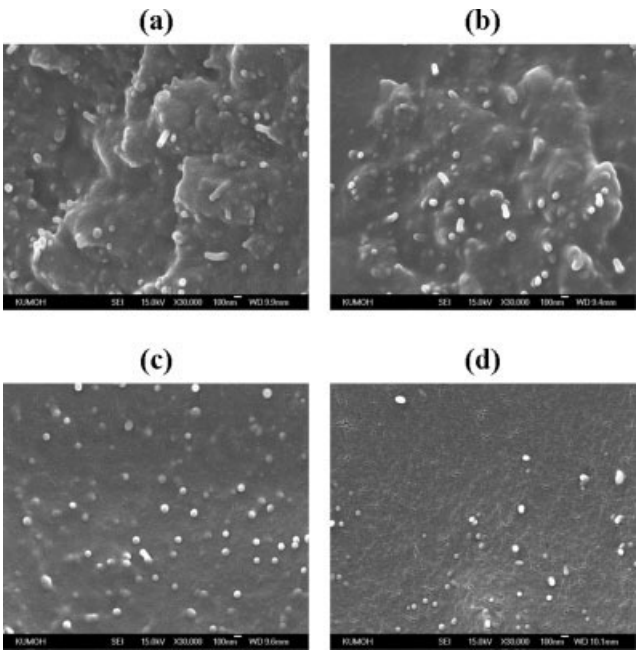

Figure 3 SEM photographs of 1.5 wt % Ph3P-MWNT with different DRs. (a) 1, (b) 3, (c) 10, and (d) 16.

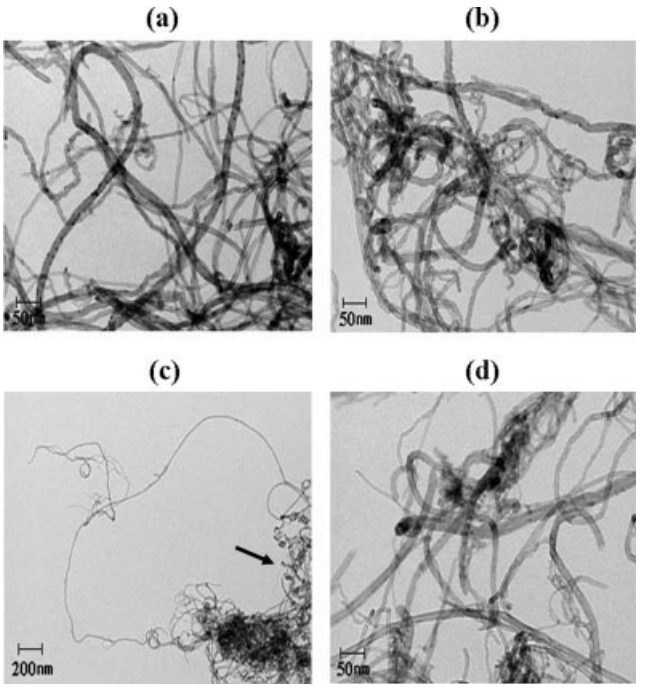

Figure 4 TEM micrographs of (a) pristine MWNT, (b) MWNT-COOH, and (c) Ph3P-MWNT. TEM micrographs of Ph3P-MWNT increasing the magnification levels from (c) to (d).

TEM images of the samples, in which all of the samples can be seen to have fewer impurities and to be much less entangled. The black dots in the figure are actually due to open MWNT ends, which means there are reactive dangling bonds. As is clear from the TEM images, the MWNTs were not broken up into small parts during the functionalization [see Fig. 4(c)]. The magnification level of the TEM micrographs of Ph3P-MWNT increases from (c) to (d). Typical TEM images of PET hybrid fibers containing 0.5 and 1.5 wt % Ph3P-MWNT are shown in Figures 5 and 6, respectively. Figure 5 shows that Ph3P-MWNT is well dispersed in the polymer matrix at all magnification levels, although some agglomerated particles have formed. For the 1.5 wt % hybrid fiber [Fig. 6(a,b)], some of the MWNTs are well dispersed within the PET matrix, with the remainder present in agglomerations. The average diameter and length of the MWNTs in Figures 5 and 6 are 10–20 nm and 20–50 nm, respectively. The SEM and TEM results indicate that for low MWNT contents the MWNTs are well dispersed throughout the PET matrix, and agglomerated structures are evident for higher MWNT contents. The unusual thermomechanical properties of these nanocomposites are discussed in the following sections with reference to the homogeneous dispersion of the MWNTs.

In conclusion, we were able to successfully synthesize PET nanocomposites with Ph3P-MWNT via an *in situ* polymerization method. We now discuss how the characteristics of the MWNTs affect the thermal behavior and tensile mechanical properties of the Ph3P-MWNT/PET hybrid fibers.

Thermal behaviors

Table I lists the thermal properties of pure PET and fibers of its hybrids with Ph3P-MWNT, obtained through *in situ* polymerization. The glass transition temperatures (T_g) of fibers of the PET hybrids with Ph3P-MWNT are higher than that of pure PET for all Ph3P-MWNT loadings from 0.3 to 1.5 wt %. Adding 0.3 wt % Ph3P-MWNT to pure PET increases the value of T_g by 5°C (see Table I). This increase in T_g is probably due to two different factors.[24,25] First, the effect of small amounts of dispersed MWNTs on the free volume of PET is significant. Second, the con-

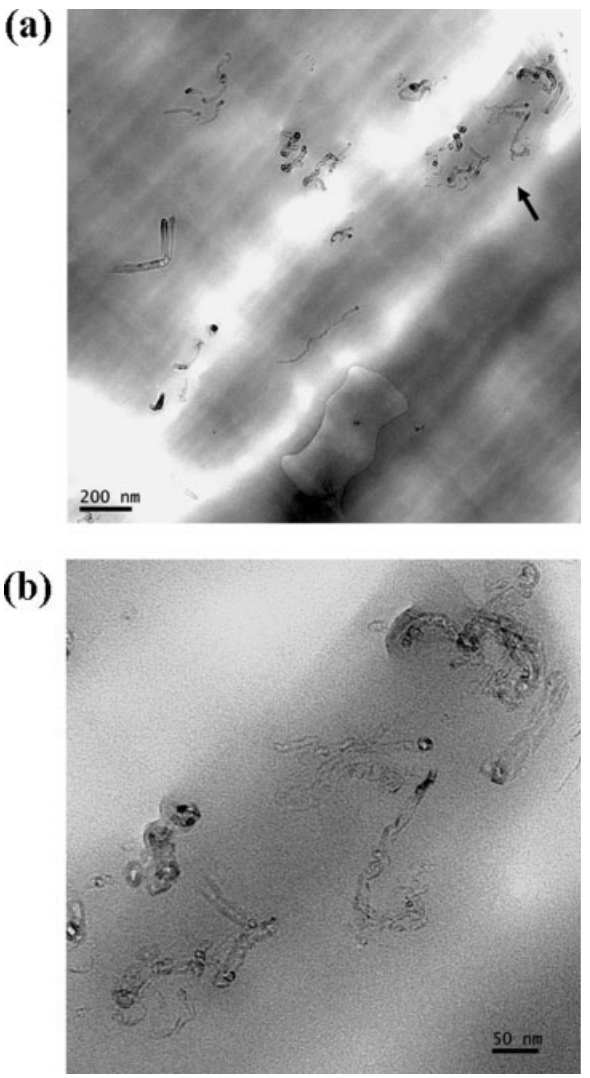

Figure 5 TEM micrographs of 0.5 wt % Ph3P-MWNT in PET hybrid fibers increasing the magnification levels from (a) to (b).

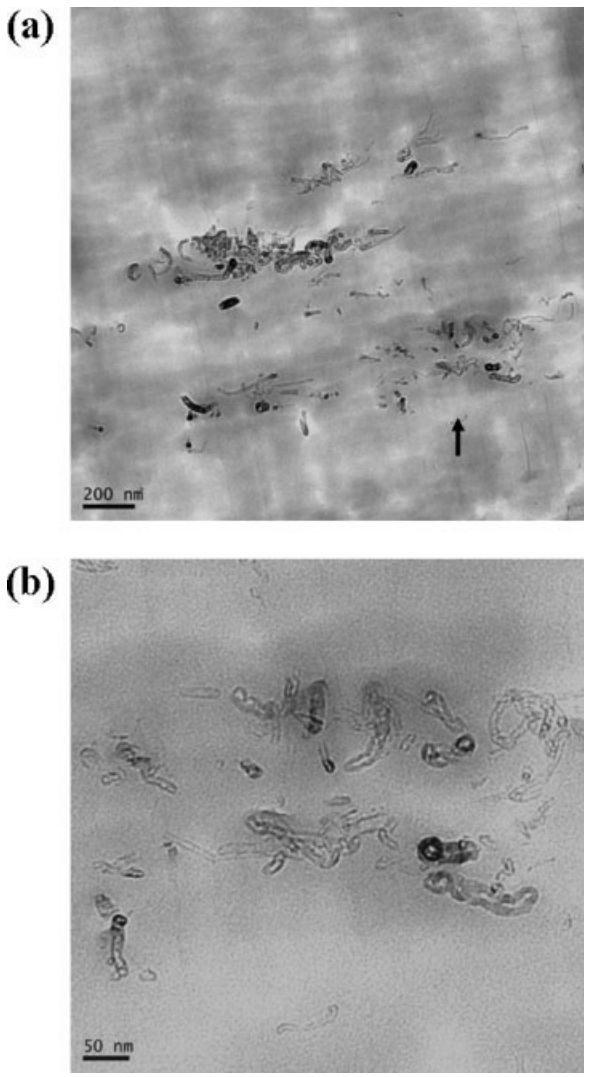

Figure 6 TEM micrographs of 1.5 wt % Ph3P-MWNT in PET hybrid fibers increasing the magnification levels from (a) to (b).

finement of dispersed polymer chains by the MWNTs limits their segmental motions.

The endothermic peak of pure PET is at 245°C, which corresponds to the melting transition temperature (T_m). The position of the maximum transition peak in DSC thermograms of the PET hybrids increases from 245 to 254°C when the Ph3P-MWNT content is increased to 0.3 wt %, and is then constant in the range 253 to 255°C when the MWNT loading is increased up to 1.5 wt % (see Table I). This increase in T_m of the hybrids might be due to the insulation effect of the MWNTs, and to interactions between the Ph3P-MWNT and PET molecular chains.[26] The DSC traces for the Ph3P-MWNT/PET hybrid fibers are shown in Figure 7.

The thermogravimetric analysis (TGA) results for the PET hybrid fibers with various Ph3P-MWNT contents are also shown in Table I. As for the results

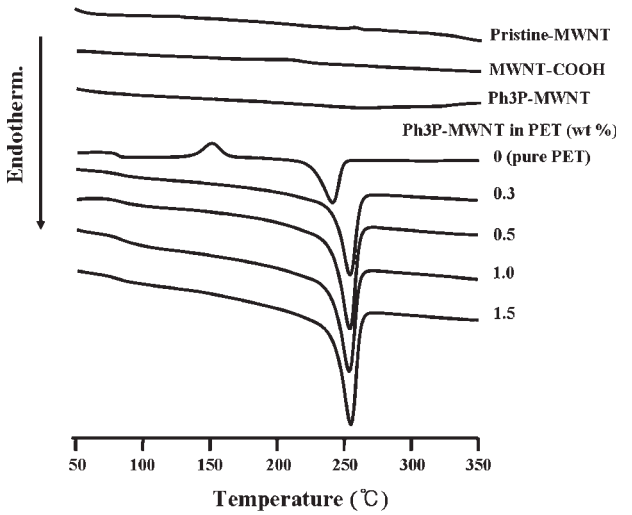

Figure 7 DSC thermograms of PET hybrid fibers with various Ph3P-MWNT contents.

for T_g and T_m, the initial thermal degradation temperatures (T_D^i) at 2% weight loss of the PET hybrids were found to be in the range 399–401°C for MWNT contents of 0.3–1.5 wt %, with a maximum increase of 31°C in the case of 0.5 wt % Ph_3P-MWNT/PET with respect to that of pure PET (370°C). Thus the introduction of MWNTs into organic polymers can improve their thermal degradation stabilities; MWNTs add thermal stability to nanoscaled composites due to the high heat resistance effect of the MWNTs and the mass transport barrier they provide to the volatile products generated during thermal decomposition.[27–29] The weight of the residue at 600°C was found to increase with increases in the MWNT loading from 0 to 1.5 wt %, ranging from 1 to 17% as shown in Table I. This enhancement of char formation with increasing Ph3P-MWNT content is ascribed to the high heat resistance of the MWNTs. The TGA curves for the pristine MWNTs, MWNT-COOH, Ph3P-MWNT, and the PET hybrid

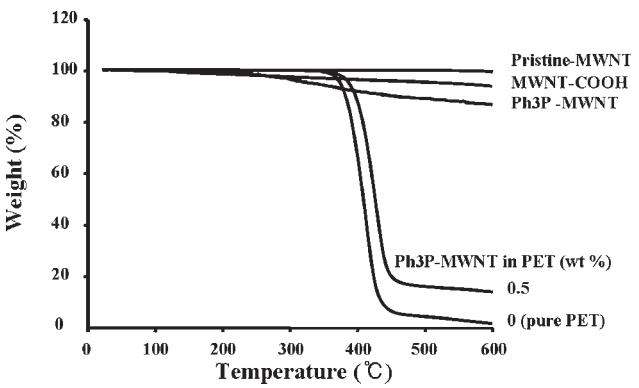

Figure 8 TGA thermograms of PET hybrid fibers with various Ph3P-MWNT contents.

TABLE II
Tensile Properties and Conductivity of Ph3P- MWNT/PET Hybrid Fibres

Ph3P-MWNT, wt %	D.R.[a]	Av.Dia.[b], μm	Ult. Str., MPa	Ini. Mod., GPa	E.B.[c], %	Conductivity, Ω/cm^2
0 (pure PET)	1	550	46	2.21	3	1.0×10^{15}
	3	278	47	2.24	3	1.0×10^{15}
	10	214	51	2.28	3	1.0×10^{15}
	16	134	51	2.39	2	1.0×10^{15}
0.3	1	605	57	2.70	2	6.26×10^{10}
	3	251	49	2.72	2	7.95×10^{10}
	10	154	46	2.95	2	8.56×10^{10}
	16	133	44	3.83	1	8.68×10^{10}
0.5	1	640	64	2.85	3	5.20×10^{10}
	3	188	54	2.91	3	4.61×10^{10}
	10	133	52	3.00	2	4.48×10^{10}
	16	114	47	4.30	1	4.45×10^{10}
1.0	1	563	60	2.89	3	5.67×10^{10}
	3	179	49	3.02	2	5.56×10^{10}
	10	155	44	3.15	2	5.07×10^{10}
	16	117	26	4.75	1	4.46×10^{10}
1.5	1	585	57	3.14	3	6.12×10^{10}
	3	189	47	3.15	2	5.61×10^{10}
	10	176	41	3.20	2	5.29×10^{10}
	16	99	26	4.91	1	4.81×10^{10}

[a] Draw ratio.
[b] Average diameter.
[c] Elongation percent at break.

fibers with various functionalized MWNT contents are shown in Figure 8.

We conclude from the above results that the introduction of functionalized MWNTs into organic polymers can improve their thermal properties. For this hybrid system, the thermal properties (T_g, T_m, and T_D[i]) of the hybrids improve with increases in the Ph3P-MWNT content up to 0.3 wt %, and then remain constant with further increases in the Ph3P-MWNT loading.

Mechanical properties

Pure PET and the PET hybrids were extruded through a capillary die with various DRs to determine the tensile strengths and moduli of the extrudates. The tensile mechanical properties of PET and its hybrids are presented in Table II. At DR = 1, the ultimate tensile strengths of the Ph3P-MWNT hybrid fibers increase with the addition of MWNT up to a critical loading, and then decrease above that critical content. For example, the strength of 0.5 wt % Ph3P-MWNT/PET hybrid fibers is 64 MPa, which is about 40% higher than that of pure PET (46 MPa). When the amount of Ph3P-MWNT in the PET hybrids reaches 1.5 wt %, the strength decreases to 57 MPa. This decrease in ultimate strength is mainly due to the agglomeration of MWNTs above the critical MWNT loading. In contrast, the initial modulus values were found to increase linearly with increases in the Ph3P-MWNT content. For a functionalized MWNT content of 1.5 wt %, the modulus of the hybrid was found to be 3.14 GPa, about 1.4 times that of pure PET (2.21 GPa).

This improvement in the tensile properties of the hybrid fibers with respect to those of pure PET is due to the presence of Ph3P-MWNT, and can be explained as follows. Note that the improvements in the tensile properties depend on the interactions between the PET polymer molecules and the functionalized MWNTs, and on the rigid nature of the MWNTs. Moreover, the MWNTs are much more rigid than, and so do not deform or relax as much as, the PET molecules. Thus these improvements arise because the functionalized MWNTs are dispersed and intercalated within the PET matrix. This is consistent with the general observation that the introduction of MWNTs into a matrix polymer increases its strength and modulus.[10,30,31]

As Table II shows, the variations with DR in the tensile strength and the initial modulus were found to be insignificant for pure PET, as is usually the case for flexible coil-like polymers. For pure PET, the strength and modulus were found to increase as the draw ratio was increased from 1 to 16, from 46 to 51 MPa, and 2.21 to 2.39 GPa, respectively. For the PET hybrid fibers, the ultimate strengths of the hybrid fibers decrease with increases in DR, as shown in Table II. For example, for a hybrid fiber with a functionalized MWNT content of 0.3 wt %, increasing DR from 1 to 16 results in a decrease in the tensile strength from 57 to 44 MPa. Similar trends were observed for hybrid fibers with Ph3P-MWNT contents of 0.5, 1.0, and 1.5 wt %.

Increases in the tensile strength with increases in DR is very common in engineering plastics and is usually observed for flexible coil-like polymers.[32–34] However, our system does not follow this trend. The observed decline in the tensile properties seems to be due to debonding between the MWNTs and the matrix polymer, and to the presence of the many nanosized voids that result from excess stretching of the fibers. This indicates that hydrostatic elongation during the extrusion and compression molding operations results in debonding in the polymer chain as well as in void formation around the polymer-MWNT interfaces.[35,36] The variations of the ultimate strengths with DR are shown in Figure 9. In contrast to the decrease in tensile strength values, the initial moduli were found to increase linearly with increases in DR for all Ph3P-MWNT contents, as shown in Figure 10. This enhancement of the modulus could be the result of two different factors: the high resistance of the MWNTs, and the orientation and aspect ratio of the MWNTs. Further, increasing the MWNT content increases the constraints on polymer chain mobility, which also increases the modulus.

The elongation at break of the hybrids was found to be virtually constant, remaining in the range 1–3% as DR was increased from 1 to 16. These values were found to be constant for Ph3P-MWNT loadings in the range 0.3–1.5 wt %. This result is characteristic of materials reinforced with stiff MWNT materials.

Previous work[37] in our laboratory has demonstrated the possibility of a reinforcing effect in PET hybrids with various organoclay contents. In contrast to the results for the PET hybrid fibers containing 1–5 wt % organoclay with increases in DR from 1 to 16, similar results in functionalized-MWNT/PET hybrid fibers were observed for all hybrids.

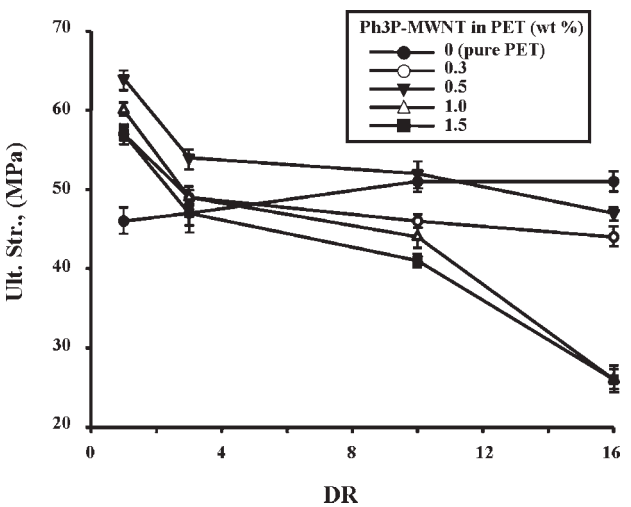

Figure 9 Effects of Ph3P-MWNT contents on the ultimate tensile strength of PET hybrid fibers.

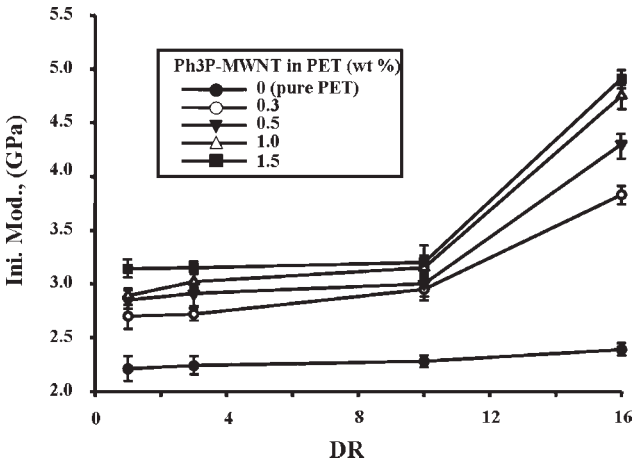

Figure 10 Effects of Ph3P-MWNT contents on the initial tensile modulus of PET hybrid fibers.

Electrical conductivity

Table II also lists the electrical conductivities of the hybrids at room temperature. The electrical conductivities of the PET hybrids increase from 1.0×10^{15} to 6.26×10^{10} as the Ph3P-MWNT content is increased to 0.3 wt %, and is constant in the range 5.20×10^{10} to 6.12×10^{10} when the MWNT loading is increased up to 1.5 wt %. These increases are due to the high aspect ratio of the MWNTs, which is associated with the overlapping of the carbon tubes. The properties of these MWNTs appear to be typical of those of highly structured and extended materials.[6,16,38] These morphological features are responsible for the large effective volume and improved connections between MWNTs.

Table II also shows the variation in the electrical conductivity with DR for the PET hybrid fibers. The stretching of carbon filler and polymer composites typically causes the separation of conductive particles and the breakage of a number of conductive paths, because the total area of contact between the conductive fillers decreases, so the electrical conductivity decreases. However, the conductivities of these materials were found to be virtually unchanged by variation in DR. For example, the electrical conductivities of the hybrid fibers containing 0.3–1.5 wt % Ph3P-MWNT were found to be independent of increases in DR from 1 to 16 (see Table II). This suggests that the dense networks of MWNTs in the Ph3P-MWNT/PET hybrid fibers retain sufficient conductive paths under increased stretching of the fibers.

CONCLUSIONS

We prepared a series of PET hybrid fibers with Ph3P-MWNT via the *in situ* polymerization method. Hybrids with various Ph3P-MWNT contents were

extruded with various DRs from a capillary rheometer to investigate their thermomechanical properties, morphologies, and conductivities.

Overall, the addition of only a small amount of Ph3P-MWNT was found to be sufficient to improve the thermomechanical properties and conductivity of the PET hybrid fibers at DR = 1. Further, when DR was increased from 1 to 16, the presence of Ph3P-MWNT in the PET matrix results in linear decreases in the ultimate tensile strengths of the hybrids due to debonding around the polymer-MWNT interfaces and void formation. There were, however, increases in the initial modulus with increases in DR. The electrical conductivities of the hybrid fibers containing 0.3–1.5 wt % Ph3P-MWNT were found to be independent of increases in DR from 1 to 16.

References

1. Giannelis, E. P. Adv Mater 1996, 8, 775.
2. Wang, D.; Zhu, J.; Yao, Q.; Wilkie, C. A. Chem Mater 2002, 14, 3837.
3. LeBaron, P. C.; Wang, Z.; Pinnavaia, T. J Appl Clay Sci 1999, 12, 11.
4. Kobayashi, H.; Shioya, M.; Tanaka, T.; Irisawa, T.; Sakurai, S.; Yamamoto, K. J Appl Polym Sci 2007, 106, 2007.
5. Shin, D. H.; Yoon, K. H.; Kwon, O. H.; Min, B. G.; Hwang, C. I. J Appl Polym Sci 2006, 99, 900.
6. Chang, T.-E.; Kisliuk, A.; Rhodes, S. M.; Brittain, W. J.; Sokolov, A. P. Polymer 2006, 47, 7740.
7. Moniruzzaman, M.; Winey, K. I. Macromolecules 2006, 39, 5194.
8. Tjong, S. C. Mater Sci Eng 2006, R53, 73.
9. Bryning, M. B.; Islam, M. F.; Kikkawa, M.; Yodh, A. G. Adv Mater 2005, 17, 1186.
10. Schadler, L. S.; Giannaris, S. C.; Ajayan, P. M. Appl Phys Lett 1998, 73, 3842.
11. Gong, X.; Liu, J.; Baskaran, S.; Voise, R. D.; Young, J. S. Chem Mater 2000, 12, 1049.
12. Ouyang, M.; Huang, J.-L.; Lieber, C. M. Acc Chem Res 2002, 35, 1018.
13. Park, S. J.; Cho, M. S.; Lim, S. T.; Choi, H. J.; Jhon, M. S. Macromol Rapid Commun 2003, 24, 1070.
14. Jia, Z.; Wang, Z.; Xu, C.; Liang, J.; Wei, B.; Wu, D.; Zhu, S. Mater Sci Eng 1999, A271, 395.
15. Velasco-Santos, C.; Marinez-Hernandez, A. L.; Lozada-Cassou, M.; Alvarez-Castillo, A.; Castano, V. M. Nanotechnology 2002, 13, 495.
16. Jiang, X.; Bin, Y.; Matsuo, M. Polymer 2005, 46, 7418.
17. Sun, Y.-P.; Fu, K.; Lin, Y.; Huang, W. Acc Chem Res 2002, 35, 1096.
18. Ge, J. J.; Zhang, D.; Li, Q.; Hou, H.; Graham, M. J.; Dai, L.; Harris, F. W.; Cheng, S. Z. D. J Am Chem Soc 2005, 127, 9984.
19. Qin, S.; Qin, D.; Ford, W. T.; Resasco, D. E.; Herrera, J. E. Macromolecules 2004, 37, 752.
20. Huang, W.; Lin, Y.; Traylor, S.; Gaillard, J.; Rao, A. M.; Sun, Y.-P. Nano Lett 2002, 2, 231.
21. Holzinger, M.; Abraham, J.; Whelan, P.; Graupner, R.; Ley, L.; Hennrich, F.; Kappes, M.; Hirsch, A. J Am Chem Soc 2003, 125, 8566.
22. Kim, D. Y.; Yang, C.-M.; Park, Y. S.; Kim, K. K.; Jeong, S. Y.; Han, J. H.; Lee, Y. H. Chem Phys Lett 2005, 413, 135.
23. Ritter, P.; Scharff, P.; Siegmund, C.; Dmyatrenko, O. P.; Kulish, N. P.; Prylutskyy, Y. I.; Belyi, N. M.; Gubanow, V. A.; Komarova, L. I.; Lizunova, S. V.; Poroshin, V. G.; Shlapatskaya, V. V.; Bernas, H. Carbon 2006, 44, 2694.
24. Chang, J.-H.; Seo, B. S.; Hwang, D. H. Polymer 2002, 43, 2969.
25. Xu, H.; Kuo, S.-W.; Lee, J.-S.; Chang, F.-C. Macromolecules 2002, 35, 8788.
26. Hussain, M.; Varley, R. J.; Mathys, Z.; Cheng, Y. B.; Simon, G. P. J Appl Polym Sci 2004, 91, 1233.
27. Fornes, T. D.; Yoon, P. J.; Hunter, D. L.; Keskkula, H.; Paul, D. R. Polymer 2002, 43, 5915.
28. Fischer, H. R.; Gielgens, L. H.; Koster, T. P. M. Acta Polym 1999, 50, 122.
29. Petrovic, X. S.; Javni, L.; Waddong, A.; Banhegyi, G. J. J Appl Polym Sci 2000, 76, 133.
30. Coleman, J. N.; Khan, U.; Gunko, Y. K. Adv Mater 2006, 18, 689.
31. Liu, T.; Phang, I. Y.; Shen L. Chow, S. Y.; Zhang, W.-D. Macromolecules 2004, 37, 7214.
32. La Mantia, F. P.; Valenza, A.; Paci, M.; Magagnini, P. L. J Appl Polym Sci 1989, 38, 583.
33. Chen, T.-K.; Tien, Y.-I.; Wei, K.-H. Polymer 2000, 41, 1345.
34. Liu, X.; Wu, Q. Polymer 2001, 42, 10013.
35. Curtin, W. A. J Am Ceram Soc 1991, 74, 2837.
36. Shia, D.; Hui, Y.; Burnside, S. D.; Giannelis, E. P. Polym Eng Sci 1987, 27, 887.
37. Chang, J.-H.; Mun, M. K. Polym Int 2007, 56, 57.
38. Kharchenko, S. B.; Douglas, J. F.; Obrzut, J.; Grulke, E. A.; Migler, K. B. Nat Mater 2004, 3, 564.